CANADIAN JOURNAL OF UROLOGY

Tech Science Press

Doi:10.32604/cju.2026.079668
ARTICLE

An in vitro, proof of concept study utilizing a latex model to simulate assessment of urethral pressure profile to quantify tissue compliance and stricture detection

Diboro L. Kanabolo,[1*] Noah Roselli,[2] Emily Ji,[1] Yashwanth Nanda Kumar,[3] Neelesh A. Patankar,[4] Ziho Lee[1]

[1]Department of Urology, Northwestern Memorial Hospital, Chicago, IL, USA
[2]Department of Engineering Sciences and Applied Mathematics, Northwestern University, Chicago, IL, USA
[3]Center for Industrial and Medical Ultrasound, Applied Physics Laboratory, University of Washington, Seattle, WA, USA
[4]Department of Mechanical Engineering, Northwestern University, Chicago, IL, USA

KANABOLO DL, ROSELLI N, JI E, KUMAR YN, PATANKAR NA, LEE Z. An *in vitro*, proof of concept study utilizing a latex model to simulate assessment of urethral pressure profile to quantify tissue compliance and stricture detection. *Can J Urol* 2026;33(4):951–958.

Background: *Retrograde urethrogram (RUG) remains the gold standard for diagnosing urethral stricture disease, however no widely available diagnostic modality currently quantifies stricture characteristics using cross-sectional area or tissue compliance. We hypothesized that pressure-derived metrics could improve diagnostic accuracy and guide treatment. We aimed to develop an in vitro latex urethra model to simulate "healthy" and "strictured" states and directly measure luminal pressure as an initial step toward compliance assessment.*
Methods: *Ten 20-cm latex tubes were studied; five contained 1.5-cm simulated strictures. All tubes were clamped at both ends to prevent leakage. Strictures were created by clamping across an 8Fr bougie at the midpoint, while healthy models were left unclamped at the 8Fr bougie location. Tubes were pressurized for 10 s to simulate RUG conditions. Pressure was measured using a 7Fr air-charged dual-sensor urodynamic catheter positioned such that the midpoint stricture was located 2 cm distal to the first pressure sensor. Saline was infused at 20 mL/min through the catheter port positioned proximal to the stricture, and maximum pressure (P_{max}, cmH_2O) was selectively recorded only from the first proximal sensor to reflect upstream resistance generated by the narrowing. Time to maximum pressure (T_{max}, seconds) was also measured. Compliance was calculated ($\Delta V/\Delta P$). Comparisons were performed using an unpaired Student's t-test.*
Results: *Ten pressure–time curves were generated. Mean (Standard Deviation) P_{max} was significantly higher in strictured models compared to healthy controls (160.8 [9.4] vs. 29.8 [16.4] cmH_2O, $p < 0.001$). T_{max} was similar between groups (9.2 [1.1] vs. 9.8 [0.4] s, $p = 0.289$). Compliance was lower in strictured (0.019 [0.003] cm^3/cmH_2O) vs. healthy tubes (0.150 [0.107] cm^3/cmH_2O, $p = 0.025$).*
Conclusions: *This proof-of-concept model demonstrates that pressure profiling can distinguish healthy from strictured urethras and supports compliance as a novel diagnostic metric.*

Key Words: urethral stricture, compliance, pressure, benchtop

Received date 11 February 2026
Accepted for publication 20 May 2026
Published online 21 August 2026

*Corresponding Author: Diboro L. Kanabolo.
Email: diboro.kanabolo@nm.org

Introduction

Urethral stricture disease represents a common and clinically significant urologic condition, affecting an estimated 0.6–1.0% of men worldwide and accounting for substantial healthcare utilization and morbidity.[1–3] The condition arises from a broad range of etiologies, including iatrogenic injury, trauma, inflammatory conditions, infection, and prior urethral surgery.[4] Regardless of cause, progressive narrowing of the urethral lumen leads to obstructive lower urinary tract symptoms, recurrent urinary tract infections, acute urinary retention, and, in severe cases, upper tract deterioration and renal dysfunction.[5,6] Despite advances in reconstructive techniques, the diagnostic evaluation of anterior urethral strictures has remained largely unchanged.[4]

Retrograde urethrography (RUG), often combined with voiding cystourethrography, remains the clinical gold standard for anatomic assessment.[7] While RUG provides information regarding the structure location and approximate length, its limitations are well recognized. The examination is operator-dependent, sensitive to contrast injection pressure and positioning, and restricted to a two-dimensional projection of a deformable structure.[8,9] Studies demonstrate that RUG frequently underestimates true stricture length and may inadequately characterize severity, particularly in dense spongiofibrosis or long-segment disease.[9–11] Furthermore, RUG provides no direct information regarding tissue composition, stiffness, or dynamic response to deformation—factors central to stricture behavior and treatment durability.[4,12]

These limitations are clinically consequential. While stricture length and location guide treatment selection, outcomes following endoscopic management, such as dilation or direct vision internal urethrotomy (DVIU), are highly variable.[13–15] Increasing evidence suggests that success is determined less by luminal caliber alone and more by biomechanical properties of the urethral wall, particularly fibrosis, stiffness, and loss of compliance.[12,16] Two strictures with similar radiographic appearance may behave differently in response to dilation, yet current tools provide no objective means of distinguishing them.[14] As a result, treatment decisions are often empirical, contributing to repeated interventions with diminishing returns and delayed urethroplasty.[13,15]

Advances in biomechanics and fluid–structure interaction modeling demonstrate that pressure–volume relationships in compliant tubular organs are robust indicators of obstruction.[17–19] In vascular, gastrointestinal, and pulmonary systems, compliance metrics integrate geometric narrowing and wall stiffness, often outperforming static imaging.[19–21] Applied to the urethra, these metrics may quantify obstruction severity while reflecting both anatomic and tissue-level pathology (Figure 1).[12,22]

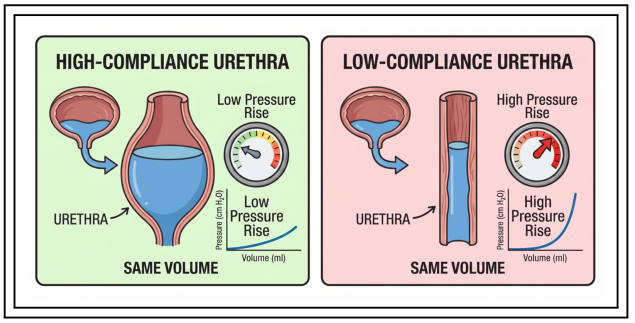

FIGURE 1. Comparative hydrodynamics of high- vs. low-compliance urethral tissue. The diagram illustrates the relationship between fluid volume and intraluminal pressure. Left: In a high-compliance urethra, the tissue is distensible, allowing for the accommodation of fluid volume with a minimal rise in pressure. Right: In a low-compliance urethra, the tissue is rigid or fibrotic; the introduction of an identical fluid volume results in a significant and rapid increase in pressure, as demonstrated by the steep trajectory of the pressure-volume curve (Original image. Created using Gemini 3.1 Pro. Google LLC. (2026). 9 May 2026)

Despite this promise, no widely accepted clinical modality exists to measure urethral compliance *in vivo*, and no validated benchtop platform has been established to study pressure–deformation dynamics in controlled healthy versus strictured states.[23] Prior work in urethral pressure profilometry and urodynamics has focused on continence rather than fixed anterior obstruction, leaving a critical gap.[23–25]

Materials and Methods

Model construction and experimental design

An *in vitro* urethral model was constructed using ten commercially available latex tubes (Natural Generic Latex, Beaimuxi, Shijiazhuang City, Hebei Province, China), each measuring 20 cm in length with an inner diameter of 1/4 inch and an outer diameter of 3/8 inch. Latex was selected as the base material due to its isotropic elastic properties, high extensibility, and well-characterized elastic modulus, allowing predictable deformation under pressurization. While latex does not fully replicate the

anisotropic, multilayered structure of native urethral tissue, its mechanical behavior provides a reproducible approximation of compliant soft tissue suitable for proof-of-concept experimentation.

Each tube was fitted with adjustable clamps at both proximal and distal ends to create a closed hydraulic system and prevent leakage during pressurization. Care was taken to ensure consistent clamp positioning and seal integrity across all trials to minimize variability in baseline pressure conditions.

Two experimental conditions were established: simulated strictured urethras (n = 5) and simulated healthy urethras (n = 5). Strictures were standardized to a length of 1.5 cm, reflecting a clinically common short-segment anterior urethral stricture. Obstruction was simulated by placing an 8 French (Fr) bougie centrally within the lumen and applying an external clamp across the tube at the stricture segment. Consistent clamp position was indicated by ensuring the clamp was placed consistently at the midpoint (10 cm mark). The same hemostat was used and utilized the same clamping pressure (one click) for all experiments to maintain consistency of pressure. This method produced a reproducible reduction in effective cross-sectional area while preserving luminal continuity and avoiding complete occlusion.

Healthy urethra models were created by inserting the same 8 Fr bougie without applying external compression, thereby controlling for catheter presence while preserving the native internal diameter of the latex tube (Figure 2). This design ensured that observed pressure differences were attributable to luminal constriction rather than instrumentation alone.

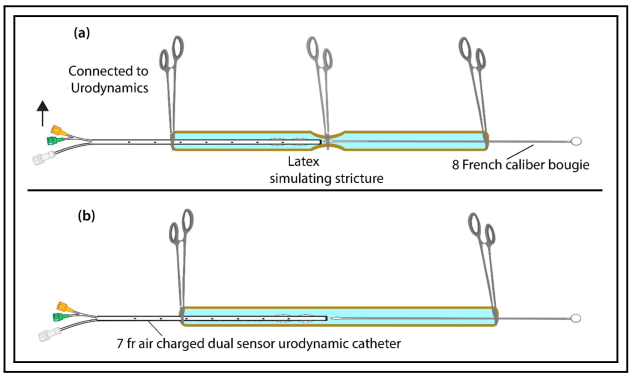

FIGURE 2. Depiction of experimental apparatus. (a): Illustration of latex urethra clamped at each end, secured to a urodynamics catheter to measure pressure (cmH_2O) within the lumen of the urethra. The 1.5 cm "stricture" is simulated by a clamp across the midpoint of the urethra. Pressure is monitored over 10 s when tubes are infilled at a rate of 20 mL/minute. (b): Similar schematic, without a clamp at the midpoint, simulating a "healthy" urethra. (Original image. Created using Adobe Illustrator 2026 (version 30.0). Adobe, Inc. (2026). 1 November 2025)

Pressurization protocol

Each tube was connected to a standard urodynamic infusion system and filled with room-temperature isotonic saline. Infusion was performed using a calibrated urodynamics pump (Nxt Pro, Laborie Medical Technologies Corp., Portsmouth, NH, USA) at a constant arbitrary rate of 20 mL/min. This rate was selected to approximate contrast injection during clinical retrograde urethrography.

Pressurization was conducted over a fixed 10-s interval, corresponding to the typical dwell time of contrast injection during RUG imaging. This standardized protocol allowed direct comparison of pressure responses across experimental conditions.

Pressure measurement and data acquisition

Intraluminal pressure was recorded using a 7 Fr air-charged dual-sensor urodynamic catheter (T-DOC Air Charged Dual Sensor Catheter, Laborie, Portsmouth, NH, USA), positioned centrally within each tube. This catheter was selected for its established clinical use in our urodynamic testing. Saline was infused at 20 mL/min through the catheter port positioned proximal to the stricture, and maximum pressure (P_{max}, cmH_2O) was selectively recorded only from the first proximal sensor to reflect upstream resistance generated by the narrowing. Pressure waveforms were continuously recorded throughout the infusion cycle using proprietary Laborie urodynamic software.

To ensure consistency across experiments, all tubing was visually inspected prior to use for manufacturing defects, wall irregularities, or microtears that could affect pressurization dynamics. Tubes were preconditioned by a single low-pressure saline infusion prior to data acquisition to minimize viscoelastic hysteresis associated with initial material loading. The urodynamic pressure transducer was zeroed to atmospheric pressure before each trial, and catheter positioning was confirmed to be centrally located within the lumen and equidistant from the proximal and distal clamps.

Each experimental run was performed at ambient laboratory temperature, and the saline temperature was maintained at room temperature to avoid viscosity-related variability in flow characteristics. Infusion tubing length and configuration were kept

constant across all trials to ensure uniform hydraulic resistance upstream of the model. Following each experiment, the system was fully depressurized and flushed with saline prior to the subsequent trial to prevent residual pressure artifacts.

All measurements were performed by the same operator using an identical experimental sequence to reduce inter-operator variability. Pressure traces were reviewed independently by two investigators to confirm waveform consistency and exclude anomalous recordings. No trials required exclusion due to technical failure, catheter malfunction, or leakage, supporting the reproducibility and stability of the experimental setup.

Model assumptions and experimental scope

This experimental model was designed to isolate pressure–deformation behavior under controlled conditions and therefore incorporates several simplifying assumptions. Latex tubing was treated as a homogeneous, isotropic elastic material, and active smooth muscle tone, anisotropic fiber orientation, and periurethral support structures were not modeled. The system was pressurized under steady infusion rather than dynamic voiding to reduce confounding variables and allow direct comparison between experimental conditions. While these assumptions limit direct physiologic equivalence, they permit reproducible assessment of relative pressure and compliance differences attributable to luminal obstruction alone, which was the primary objective of this proof-of-concept study.

Outcome measures

Primary outcome measures included maximum intraluminal pressure achieved (P_{max}, cmH_2O) and time to maximum pressure (T_{max}, seconds). The secondary outcome measure was compliance. This was calculated using a standardized infusion-based method, wherein the change in volume (ΔV) (cm^3/cmH_2O) was defined as the total instilled fluid at a constant rate of 20 cm^3/min up to the point of maximal pressure, and the change in pressure (ΔP) was defined as the peak pressure achieved after manual zeroing of the initial pressures.

Statistical analysis

Comparisons between strictured and healthy conditions were performed using a two-tailed unpaired Student's *t*-test. Data are presented as mean ± standard deviation (SD) unless otherwise specified. Statistical significance was defined as $p < 0.05$. Assumptions of approximate normality and variance similarity were assessed prior to applying the two-tailed Student's *t*-test, recognizing the limitations inherent to small sample sizes. All analyses were performed using GraphPad Prism version 10 (San Diego, CA, USA).

Results

Ten pressure–time curves were generated using a benchtop latex urethral model, including five healthy and five simulated strictured lumens Pressure–time curves in strictured models demonstrated relatively narrow ranges for peak pressure, supporting reproducibility under obstructed conditions. In contrast, healthy models exhibited greater variability in P_{max} (range 10–54 cmH_2O; SD 16.4), likely reflecting increased sensitivity of low-pressure measurements to minor experimental factors such as air bubbles, subtle differences in tube compliance, or leakage. Strictured models exhibited markedly higher peak intraluminal pressures and substantially reduced compliance compared with healthy models, while time to peak pressure did not differ significantly between groups (Table 1).

Peak intraluminal pressure differed markedly between experimental conditions. Strictured urethra models demonstrated a mean (SD) P_{max} of 160.8 (9.4) cmH_2O, compared with 29.8 (16.4) cmH_2O in healthy models ($p < 0.001$). This represented more than a fivefold increase in peak pressure under identical infusion conditions.

Time to peak pressure did not differ significantly between groups. Strictured models reached maximal pressure at a mean (SD) of 9.2 (1.1) s, whereas healthy models reached peak pressure at 9.8 (0.4) s ($p = 0.289$), indicating a similar duration of the filling phase between groups, rather than similar overall filling dynamics.

Compliance analysis further distinguished the two states. Strictured tubes exhibited markedly reduced compliance (0.019 [0.003] cm^3/cmH_2O) compared with healthy tubes (0.150 [0.107] cm^3/cmH_2O), $p = 0.025$ representing a near 8-fold difference in volumetric distensibility.

Discussion

This benchtop study suggests that pressure-derived metrics can objectively discriminate between "healthy" and "strictured" urethral states, supporting the hypothesis that luminal compliance represents a quantifiable biomechanical signature of urethral

TABLE 1. **Pressure–time characteristics of healthy versus strictured latex urethra models**

Parameter	Healthy urethra (n = 5)	Strictured urethra (n = 5)	*p* value
Peak intraluminal pressure, P_{max} (cmH_2O), mean (SD)	29.8 (16.4)	160.8 (9.4)	<0.001
P_{max} range (cmH_2O)	10–54	149–173	—
Time to peak pressure, T_{max} (s), mean (SD)	9.8 (0.4)	9.2 (1.1)	0.289
T_{max} range (s)	9–10	8–10	—
Compliance, $\Delta V/\Delta P$ (cm^3/cmH_2O)	0.150 (0.107)	0.019 (0.003)	0.025

Note. "—" indicates not applicable/not evaluated.

obstruction. While retrograde urethrography remains the clinical gold standard for anatomic assessment, its limitations are well established. These include operator dependence, two-dimensional representation, and systematic underestimation of structure length.[7–9] Conventional imaging provides no information regarding tissue stiffness or dynamic response to deformation, increasingly recognized as central to stricture behavior and treatment durability.[4,12]

Prior efforts to characterize urethral obstruction using pressure-based approaches have largely emerged from the urodynamics literature rather than reconstructive diagnostics. Early studies evaluating urethral pressure profilometry focused primarily on continence mechanisms and sphincteric function rather than fixed anterior urethral obstruction.[23,24] However, these investigations demonstrated that localized pressure elevations along the urethral axis can reflect functional resistance and wall interaction, laying conceptual groundwork for pressure-based assessment.

Experimental and preclinical models have begun to reintroduce pressure profiling as a means of assessing urethral biomechanics more directly. Prior work has demonstrated that compliance-related parameters measured using ultrasound and flow metrics could distinguish fibrotic from non-fibrotic urethral segments in preclinical models, reinforcing the concept that tissue stiffness—not simply luminal diameter—drives functional obstruction.[12,16] Advances in elastography and soft-tissue biomechanics across multiple hollow-organ systems further support this paradigm.[18–20] The present study builds on this body of work by isolating intraluminal pressure as a primary signal and demonstrating that, even in a simplified benchtop model, pressure kinetics alone can robustly differentiate strictured from non-strictured states.

From a clinical standpoint, the ability to quantify urethral compliance may address one of the most persistent challenges in stricture management: predicting which strictures are amenable to endoscopic therapy versus those likely to fail.[13–15] Low-compliance strictures are expected to resist radial expansion despite aggressive dilation, explaining the poor durability observed clinically, whereas higher-compliance strictures may reflect less fibrotic disease and better endoscopic candidacy.[16]

While variability in the healthy control group was proportionally greater than expected for a standardized *in vitro* model, values were verified and no typographical error was identified. We suspect this variability may reflect minor experimental artifacts inherent to low-pressure systems, including small differences in tube compliance, incomplete elimination of air bubbles, microscopic leakage at clamp interfaces, or subtle variation in catheter positioning relative to the infusion stream.

In our model, strictured segments exhibited nearly a five-fold increase in peak intraluminal pressure compared with healthy lumens under identical infusion conditions, while time to peak pressure remained similar. This suggests that resistance to radial expansion, rather than delayed filling or altered flow timing, is the dominant biomechanical feature distinguishing the two states. These findings are consistent with fluid–structure interaction principles observed in other tubular systems, where reduced compliance manifests as disproportionate pressure elevation without significant changes in temporal flow characteristics.[17–19] Importantly, pressure-based metrics integrate both geometric narrowing and wall stiffness, offering a more comprehensive functional assessment than static imaging alone.[11,18]

Clinical interpretation and decision-making implications

From a clinical standpoint, the ability to quantify urethral compliance may address one of the most persistent challenges in stricture management: predicting which strictures are amenable to endoscopic therapy versus those that are destined to fail. Current decision-making relies heavily on structure length, location, and prior treatment history, yet these parameters incompletely capture the biological severity of disease. Dense spongiofibrosis, which limits tissue distensibility, may be present even in relatively short strictures and is not reliably appreciated on standard imaging.[4,12] As a result, patients with similar radiographic findings may experience dramatically different outcomes following dilation or direct vision internal urethrotomy.[13–15]

A pressure-derived compliance metric has the potential to function as an objective surrogate for underlying fibrosis. Low-compliance strictures, characterized by steep pressure–volume relationships, would be expected to resist radial expansion despite aggressive dilation, explaining the poor durability observed clinically. Conversely, higher-compliance strictures may reflect less fibrotic disease with preserved elasticity, identifying a subgroup of patients more likely to benefit from minimally invasive intervention. Incorporating compliance measurements into preoperative evaluation could therefore improve patient selection, reduce futile endoscopic procedures, and support earlier referral for definitive urethroplasty when appropriate.[14,16]

Such an approach aligns with broader trends in functional urologic diagnostics, where physiologic measurements increasingly complement anatomic imaging. Analogous paradigms exist in vascular medicine, where pressure gradients and compliance indices guide intervention beyond angiographic stenosis alone, and in gastroenterology, where manometric and compliance-based testing inform management of obstructive disorders.[18–21] Applying similar principles to urethral stricture disease represents a natural evolution toward physiology-informed reconstructive decision-making.

Implications for diagnostic paradigms and technology development

Beyond individual treatment decisions, pressure-based urethral assessment may enable a broader shift in how stricture disease is conceptualized and staged. Rather than classifying strictures solely by length and location, future diagnostic frameworks could incorporate biomechanical phenotypes defined by compliance, stiffness, and pressure response. Such phenotyping may help explain variability in disease progression, recurrence patterns, and response to therapy, and could serve as a foundation for more personalized treatment algorithms.[20,21]

From a technological perspective, the findings of this study support ongoing development of catheter-based and endoscopic pressure-sensing platforms capable of capturing localized urethral pressure profiles *in vivo*. Advances in miniaturized sensors, wireless telemetry, and real-time signal processing raise the possibility of integrating pressure measurement into routine diagnostic cystoscopy or retrograde studies with minimal added procedural burden. Coupled with imaging modalities such as ultrasound or fluoroscopy, pressure-derived data could enable combined geometric and biomechanical mapping of urethral pathology.[22]

Furthermore, pressure–compliance data generated *in vivo* could inform computational fluid–structure interaction models, allowing simulation of patient-specific urethral behavior under physiologic voiding conditions. Such models may ultimately support surgical planning, graft selection, and reconstruction strategy by predicting functional outcomes based on individualized tissue mechanics.[17–19]

Importantly, the integration of biomechanical metrics into urethral stricture evaluation aligns with emerging efforts to standardize outcome assessment in reconstructive urology. Recent frameworks such as *StrictureFecta* emphasize the need for multidimensional evaluation incorporating not only anatomic patency but also functional and patient-centered outcomes. In this context, pressure-derived parameters such as compliance and peak pressure may offer objective, quantifiable measures of functional obstruction that complement existing criteria. Incorporation of such metrics into standardized reporting frameworks may enhance comparability across studies, improve treatment stratification, and facilitate more rigorous assessment of therapeutic success.[26]

Limitations and model interpretation

While this study establishes proof of concept, important limitations warrant emphasis. The latex model employed here represents a simplified approximation of urethral mechanics and does not replicate the layered architecture, anisotropic collagen alignment, or active smooth muscle tone present in native tissue. Incorporation of graded stenosis severity and length would provide valuable insight into potential dose–response or monotonic relationships between

luminal narrowing and derived metrics. This represents an important direction for future work. *In vivo*, urethral compliance reflects a complex interplay between epithelium, spongiosum, fibrosis, and surrounding structures, which cannot be fully captured in a benchtop system.[12,18]

Additionally, strictures were modeled as uniform, externally applied constrictions rather than heterogeneous fibrotic lesions with variable stiffness along their length. Pressurization occurred under controlled infusion rather than dynamic voiding, and compliance estimates in healthy tubes relied partly on known material properties and artificial cutoff in infusion volumes, rather than direct volumetric measurement in higher fidelity simulated models. Future studies involving *ex vivo* tissue models (e.g., porcine urethra) are necessary to better capture anisotropic, viscoelastic, and multilayer tissue properties not represented in the current latex model. Given the small sample size ($n = 5$ per group), statistical comparisons are underpowered and should be considered exploratory. Despite these limitations, the magnitude and consistency of pressure separation observed between experimental conditions support the validity of pressure kinetics as a discriminative signal and justify further translational investigation.

Conclusion

This study provides foundational evidence that pressure profiling and compliance measurement offer a novel, quantitative framework for evaluating urethral obstruction. Using a controlled *in vitro* model, we demonstrate that strictured lumens exhibit markedly elevated peak pressures and substantially reduced compliance compared with healthy counterparts under identical pressurization conditions. These findings support the concept that urethral obstruction cannot be fully characterized by anatomic narrowing alone and that tissue biomechanics play a central role in functional severity.

By introducing a reproducible platform for studying urethral pressure–deformation relationships, this work establishes a critical bridge between engineering principles and reconstructive urology. Compliance-based assessment has the potential to augment existing imaging modalities, improve prediction of endoscopic treatment durability, and guide more informed selection of definitive surgical intervention. This approach aligns with broader shifts toward physiology-informed diagnostics across multiple medical disciplines. Beyond its immediate findings, this work highlights the importance of incorporating functional biomechanical metrics into the evaluation of urethral disease. Pressure-derived measures offer a scalable and potentially generalizable framework that could be adapted to a wide range of structural phenotypes, including variations in length, location, and underlying tissue composition. As diagnostic technologies evolve, such metrics may be integrated into catheter-based systems, endoscopic workflows, or intraoperative assessment tools, enabling real-time characterization of obstruction severity. Importantly, objective quantification of compliance may facilitate standardized disease classification, improve comparability across studies, and support more rigorous evaluation of novel therapeutic strategies. By establishing a reproducible experimental foundation, this study lays the groundwork for future translational efforts aimed at refining patient selection, optimizing timing of reconstruction, and ultimately improving outcomes for patients with urethral stricture disease.

While further validation in biologic tissue and *in vivo* settings is required, the results of this study provide a compelling rationale for continued development of pressure-based urethral diagnostics. Ultimately, integrating geometric imaging with pressure-derived biomechanical profiling may enable a new class of objective, patient-specific tools for urethral stricture evaluation—an approach that is currently being translated and evaluated in patients as part of our ongoing clinical investigations.

Acknowledgement

The authors thank Nicole Hall and Guerin Williams for their assistance with experimental setup and preparation.

Funding Statement

The authors received no specific funding for this study.

Author Contributions

Diboro L. Kanabolo conceived the study, performed experiments, analyzed data, and drafted the manuscript. Noah Roselli and Neelesh A. Patankar contributed to experimental design, biomechanical modeling, and interpretation of

results. Emily Ji assisted with conception and provided biomechanical modeling/experimental design insights. Yashwanth Nanda Kumar assisted with data acquisition and figure preparation. Ziho Lee provided clinical oversight, contributed to study design, and critically revised the manuscript. All authors reviewed and approved the final version of the manuscript.

Availability of Data and Materials

The datasets generated and analyzed during the current study are available from the corresponding author upon reasonable request.

Ethics Approval

This study was conducted using an *in vitro* experimental model and did not involve human participants or animals. As such, institutional review board approval was not required.

Conflicts of Interest

The authors declare no conflicts of interest.

References

1. Santucci RA, Joyce J, Wise M. Male urethral stricture disease. *J Urol* 2007;177:1667–1674.
2. Lumen N, Hoebeke P, Willemsen P et al. Etiology of urethral stricture disease in the 21st century. *J Urol* 2009;182(3):983–987. doi:10.1016/j.juro.2009.05.023.
3. Palminteri E, Berdondini E, Verze P et al. Contemporary urethral stricture characteristics. *Eur Urol* 2013;63:488–493.
4. Mundy AR, Andrich DE. Urethral strictures. *BJU Int* 2011;107(1):6–26. doi:10.1111/j.1464-410x.2010.09800.x.
5. Cabral JD, Alkassis M, Khalafalla K et al. Contemporary trends in the management of urethral stricture disease in the era of the AUA guidelines. *Urology* 2025;206:173–179. doi:10.1016/j.urology.2025.07.054.
6. Rourke KF, Jordan GH. Primary urethral reconstruction outcomes. *J Urol* 2005;173:1206–1210.
7. Maciejewski C, Rourke K. Imaging of urethral stricture disease. *Transl Androl Urol* 2015;4:2–9.
8. Harris D, Zhou C, Girardot J et al. Imaging in urethral stricture disease: an educational review of current techniques with a focus on MRI. *Abdom Radiol* 2023;48(2):1062–1078. doi:10.1007/s00261-022-03761-5.
9. McAninch JW, Laing FC, Jeffrey RB Jr. Sonourethrography in the evaluation of urethral strictures: a preliminary report. *J Urol* 1988;139(2):294–297. doi:10.1016/s0022-5347(17)42391-3.
10. Fiedler G, Bittencourt LK, Zhou C et al. Magnetic resonance imaging of the urethra. *Radiol Bras* 2023;56(6):343–345. doi:10.1590/0100-3984.2023.0084.
11. Humphrey JD. Mechanics of the arterial wall. *Crit Rev Biomed Eng* 1995;23:1–162.
12. Holzapfel GA. *Biomechanics of soft tissues*. New York, NY, USA: Springer; 2000.
13. Heyns CF, Steenkamp JW, De Kock ML et al. Treatment of male urethral strictures. *J Urol* 1998;160:356–358. doi:10.1097/00005392-199808000-00016.
14. Issack FH, Hassen SM, Tefera AT et al. Short-term recurrence rate of male urethral stricture and its predictors after treatment with optical internal urethrotomy: prospective Cohort study at a tertiary center in Ethiopia. *Ann Med Surg* 2023;85(10):4715–4719. doi:10.1097/ms9.0000000000001253.
15. Endo D, Robayo J, García-Perdomo HA. Predictors of urethral stricture recurrence following internal urethrotomy: a systematic review. *Urol J* 2025;92(1):32–38. doi:10.1177/03915603241292191.
16. Cavalcanti A, Schul A, Restrepo CF et al. Pathophysiology of urethral stricture disease. In: *Urethral reconstruction*. Cambridge, MA, USA: Academic Press, 2022.
17. Wang Z, Chesler NC. Pulmonary vascular stiffness. *Pulm Circ* 2011;1:212–223.
18. Fung YC. *Biomechanics: mechanical properties of living tissues*. 2nd ed. New York, NY, USA: Springer; 1993.
19. Kassab GS. Biomechanics of the cardiovascular system. *J R Soc Interface* 2006;3:719–740.
20. Pandolfi A, Vasta M. Fiber distributed models of biological tissues. *Mech Res Commun* 2012;40:1–5. doi:10.1016/j.mechmat.2011.06.004.
21. Hoyt K, Castaneda B, Zhang M et al. Tissue elasticity as biomarkers for prostate cancer. *Cancer Biomark* 2008;4:213–225.
22. Sarvazyan A, Hall JT, Urban WM et al. An overview of elastography—an emerging branch of medical imaging. *Curr Med Imaging Rev* 2011;7(4):255–282. doi:10.2174/157340511798038684.
23. Griffiths DJ. *Urodynamics: the mechanics and hydrodynamics of the lower urinary tract*. Bristol, UK: Adam Hilger; 1980.
24. Working Group of the United Kingdom Continence Society, Abrams P, Eustice S et al. United kingdom continence society: minimum standards for urodynamic studies, 2018. *Neurourol Urodyn* 2019;38(2):838–856. doi:10.1002/nau.23909.
25. Wessells H, Morey AF, McAninch JW et al. Male urethral stricture guideline amendment. *J Urol* 2023;210(1):64–71. doi:10.1097/ju.0000000000003482.
26. Mantica G, Verla W, Frankiewicz M et al. Toward standardized outcome reporting in urethral reconstruction: development of the "stricture-fecta" through an international modified delphi consensus. *Eur Urol Open Sci* 2026;83:120–124. doi:10.1016/j.euros.2025.11.008.